Polymer Chemistry

PAPER

View Article Online
View Journal | View Issue

Cite this: *Polym. Chem.*, 2018, **9**, 2813

Stimuli-responsive supramolecular conjugated polymer with phototunable surface relief grating†

Cheng-Wei Huang, Wen-Yu Ji and Shiao-Wei Kuo *

Received 20th March 2018,
Accepted 19th April 2018

DOI: 10.1039/c8py00439k

rsc.li/polymers

We have used a facile method to prepare azobenzene- and (bio-inspired) thymine (T)-functionalized conjugated copolymers (PTCAz-T) through Suzuki coupling polymerization and click reactions. The glass transition temperature of PTCAz-T is increased after performing the click reactions, compared with that of its precursor T-free PTCAz-N_3 conjugated copolymer, because the strong T–T interactions restricted the molecular motion, decreased the free volume, and provided a more stable morphology. The presence of the azobenzene units in the main chain of the conjugated polymer presenting the T units resulted in amorphous phase behavior without macro-phase separation, and allowed the preparation of homogeneous photo-controllable thin films exhibiting stimuli-responsive behavior through photo-induced *trans*-to-*cis* isomerization. In addition, we use the conjugated copolymer PTCAz-T to prepare surface relief gratings displaying long-range-ordered interference patterns. Thus, such materials have potential applications in optical storage media while also providing a pathway for further supramolecular development.

Introduction

Stimuli-responsive polymers have received much interest for their uses in biosensing, actuators, and drug delivery because of their unique surface properties and self-assembly behavior.[1–5] Supramolecular materials inspired by Nature are useful tools for molecular designs mediated through noncovalent interactions (*e.g.*, ionic, coordinate, and hydrogen bonds).[6–8] Hydrogen-bonded supramolecular polymers featuring DNA-like guanine (G), cytosine (C), thymine (T), and adenine (A) nucleobases have been used to prepare biomimetic materials and extend the applications of traditional polymers.[9–12]

Conjugated polymers have been used extensively in materials science; their light-emitting ability and semiconducting properties have been particularly applicable in organic photovoltaic devices, display technologies, and optical storage media.[13–17] In addition, the photoresponsive behavior of azobenzene derivatives is readily exploitable in photoswitching applications.[18–21] Azobenzene compounds can photo-isomerize reversibly, with *trans*-to-*cis* isomerization induced by UV irradiation (wavelength: *ca.* 350 nm) and *cis*-to-*trans* isomerization by harmless visible light or heat, with both processes potentially resulting in significant changes in dipole moment, visual color, and molecular orientation.[22] Such geometric changes provide azobenzene-containing materials with many applications in micropatterning, light-triggered nanocarriers, host/guest materials, and optical storage media.[23–32]

The photoresponsive behavior of azobenzene-functionalized materials can, therefore, be used for polarization holography or data storage. Accordingly, azobenzene-containing conjugated polymers are also suitable candidates for application in holographic storage.[26–32] Nevertheless, because of relatively low glass transition temperatures (T_g), some azobenzene-functionalized polymers and related compounds possess poor thermal stability, which must, therefore, be taken into account when designing responsive systems.[33] Furthermore, an additional criterion for photoinduced mass migration is a sufficiently strong interaction between the chromophore and the conjugated polymer backbone through covalent or noncovalent bonding (*e.g.*, hydrogen bonding).[34]

As a result, we prepared azobenzene- and T-functionalized conjugated polymers, through Suzuki coupling polymerization and click reactions that form stimuli-responsive materials that operate through a combination of covalent and noncovalent interactions in this study. In a previous study, we found that the light emitting ability featuring an arylamine backbone led to a remarkable enhancement.[16] Therefore, we incorporated azobenzene units in the main chain of this kind of conjugated polymer (PTC) to enhance the surface-modulation depth during *trans*-to-*cis* isomerization under UV light and, thereafter, increase the diffraction efficiency. In addition, the com-

Department of Materials and Optoelectronic Science, National Sun Yat-Sen University, Kaohsiung, 804, Taiwan. E-mail: kuosw@faculty.nsysu.edu.tw

†Electronic supplementary information (ESI) available: Chemical structures for FTIR and NMR spectra for monomers are shown in Fig. S1–S9. See DOI: 10.1039/c8py00439k

bination of stimuli-responsive azobenzene units and the strong T–T multiple hydrogen bonding interactions provided these new conjugated polymers with tunable photophysical and thermal properties. As a result, we used this approach to prepare a stimuli-responsive conjugated polymer possessing a unique surface structure that allowed the generation of a surface relief grating (SRG).

Experimental section

Materials

4-Butylaniline, 1,6-dibromohexane, 4-iodoaniline, 1-bromo-4-iodobenzene, propargyl bromide (80 wt% in toluene), and 1,10-phenathroline were purchased from Alfa. Carbazole, pentamethyldiethylenetriamine (PMDETA, 99%), 2-isopropoxytetramethyldioxaborolane, sodium azide, sodium hydroxide, T, ammonium chloride, potassium carbonate, potassium hydroxide, tetrahydrofuran (THF), CH_2Cl_2, methanol (MeOH), dimethylformamide (DMF), and acetonitrile (MeCN) were purchased from Sigma-Aldrich. *n*-Butyllithium (2.5 M in *n*-hexane) was purchased from Chemetall. 3,6-Dibromo-9*H*-carbazole, 9-(6-bromohexyl)-3,6-dibromo-9*H*-carbazole, 9-(6-azidohexyl)-3,6-dibromo-9*H*-carbazole, 4-butyl-*N*,*N*-bis(4,4,5,5-tetramethyl-1,3,2-dioxaborolane-4-phenyl)aniline, and propargyl thymine (PT) were synthesized using previously reported procedures [Schemes S1(a) and S1(b)†].[16,35–37]

(*E*)-1,2-Bis(4-iodophenyl)diazene

4-Iodoaniline (3.00 g, 13.7 mmol) was placed in a two-neck reaction flask with DCM (80 mL) and stirred under a N_2 atmosphere for 30 min. $KMnO_4$ (5.10 g, 32.2 mmol) and $CuSO_4{\cdot}5H_2O$ (5.10 g, 20.4 mmol) were added and then the mixture was stirred at room temperature for 72 h (Scheme S1(c)†). The resulting mixture was passed through silica gel to remove excess $KMnO_4$ and $CuSO_4{\cdot}5H_2O$; after concentration, the residue was purified through column chromatography (CH_2Cl_2/hexane, 1/4) and dried under the vacuum to provide an orange powder (0.54 g, 18%). FTIR (cm^{-1}): 532, 831 (C–H bending, *cis*-isomer), 1394, 1466 (C–C bending, *cis*-isomer), 556, 851 (C–H bending, *trans*-isomer), and 1415, 1490 (C–C bending, *trans*-isomer) (Fig. S7†). ^{1}H NMR (500 MHz, $CDCl_3$, δ/ppm): 7.6 (d, ArH), 7.8 (d, ArH) (Fig. S8†). ^{13}C NMR (125 MHz, $CDCl_3$, δ/ppm): 98, 125, 139, 151 (Fig. S9†).

PTCAz-N_3

9-(6-Azidohexyl)-3,6-dibromo-9*H*-carbazole (0.280 g, 0.660 mmol), 4-butyl-*N*,*N*-bis(4-(4,4,5,5-tetramethyl-1,3,2-dioxaborolan-2-yl)phenyl)aniline (0.820 g, 1.48 mmol), (*E*)-1,2-bis(4-iodophenyl)diazene (0.280 g, 0.660 mmol), Aliquat 336® (6 drops), aqueous K_2CO_3 (2 M, 2 mL), and anhydrous THF (10 mL) were placed in a flame-dried Schlenk tube. The mixture was subjected to three freeze/pump/thaw cycles. Tetrakis(triphenylphosphine)palladium (34 mg, 0.02 mmol) was added and then the mixture was heated under reflux at 65 °C for 4 days. The copolymers were precipitated by pouring the reaction mixture into a large amount of cold MeOH; they were collected, redissolved in THF, and passed through a Celite column to remove the palladium catalyst. After Soxhlet extraction with MeOH and acetone, a red-orange powder was recovered (60% yield). ^{1}H NMR (500 MHz, $CDCl_3$, δ/ppm): 7.10–8.30 (br, ArH), 4.30 (br, CH_2), 3.20 (br, CH_2N_3) 1.91 (br, CH_2), 1.50–1.05 (br, CH_2), 0.87 (br, CH_3).

PTCAz-T

A mixture of PTCAz-N_3 (0.15 g, 0.25 mmol) in anhydrous THF (10 mL), PT (0.16 g, 0.97 mmol) in anhydrous DMF (10 mL), and Cu(I)Br (3 mg) was subjected to a freeze/pump/thaw cycle. PMDETA (20 μL) was added into the reaction vessel, which was then heated at 45 °C for 24 h. The resulting mixture was passed through a column of aluminum oxide and concentrated. Three cycles of dissolving in DMF and precipitating in MeOH provided a deep-red product (90% yield). ^{1}H NMR (500 MHz, $CDCl_3$, δ/ppm): 8.23 (br, NH), 7.10–8.00 (br, ArH), 5.12 (br, CH_2), 4.88 (br, CH_2), 4.20 (br, NCH_2), 2.62 (br, CH_2), 1.65 (s, T CH_3), 1.50–1.00 (br, CH_2), 0.92 (br, CH_3).

SRG

A thin film of the dye-doped T-functionalized conjugated polymer PTCAz-T was prepared under polarized green light (532 nm) from a diode-pumped solid state (DPSS) laser at an intensity of 20 mW cm^{-2}. This laser light was collimated and then passed through a polarized beam splitter; the incident angle (3.5°) of the reference beam was maintained under the air (see Scheme 2). A transverse-electric polarized He–Ne laser beam (632 nm) was used to probe the surface grating.

Characterization

Nuclear magnetic resonance (NMR) spectroscopy was performed using an Agilent Unity Inova 500 spectrometer with DMSO-d_6 or $CDCl_3$ as the solvent. Fourier transform infrared (FTIR) spectroscopy was performed using a Bruker Tensor 27 FTIR instrument; the samples were prepared using the KBr disk method; 32 scans were recorded at a resolution of 4 cm^{-1}. Molecular weights were measured using a Waters 510 gel permeation chromatography (GPC) system equipped with three Ultrastyragel columns (100, 500, and 1000 Å) connected in series; DMF was the eluent (flow rate: 0.6 mL min^{-1}; 50 °C); DMF-insoluble polymers were characterized using THF as the eluent and equipping the instrument with a JASCO RI-2031 detector and a Styragel HR4 column. Differential scanning calorimetry (DSC) was performed using a TA Instruments Q-20 apparatus; the samples (5–8 mg) were sealed in an aluminum pan and scanned from 30 to 200 °C at a heating rate of 20 °C min^{-1} under a N_2 atmosphere. UV–Vis spectroscopy was performed using an HP 8453 diode-array spectrophotometer. Photoluminescence (PL) emission spectroscopy was performed in solution at room temperature using a Hitachi F-4500 fluorescence spectrometer and monochromatized Xe light. Atomic force microscopy (AFM) was performed using a Dimension 3100 apparatus (Digital Instrument), operated in the tapping regime mode, at room temperature.

Results and discussion

Synthesis and characterization of PTCAz-T

Scheme 1 displays the synthesis of the dye-doped T-functionalized conjugated polymer PTCAz-T through Suzuki coupling polymerization of 9-(6-azidohexyl)-3,6-dibromo-9*H*-carbazole, 4-butyl-*N*,*N*-bis(4-(4,4,5,5-tetramethyl-1,3,2-dioxaborolan-2-yl)phenyl)aniline, and (*E*)-1,2-bis(4-iodophenyl)diazene, followed by a click reaction. Fig. 1 displays the FTIR spectra of PTCAz-T, PTCAz-N_3, and PT recorded at room temperature. The characteristic peak of the C≡C unit of PT appeared at 2120 cm^{-1}, while that of the side chain azido unit of PTCAz-N_3 appeared at 2095 cm^{-1}. Both of these signals disappeared after performing the click reaction of PTCAz-N_3 with PT. The spectrum of the conjugated polymer PCTAz-T featured a signal for the C=O groups of the T units at 1680 cm^{-1}. Fig. S1–S4† present the ^1H and ^{13}C NMR spectra of 9-(6-azidohexyl)-3,6-dibromo-9*H*-carbazole and 4-butyl-*N*,*N*-bis(4-(4,4,5,5-tetramethyl-1,3,2-dioxaborolan-2-yl)phenyl)aniline. The signal of the CH_2 protons connected to the azide unit of PTCAz-N_3 appeared at 3.20 ppm (peak c, Fig. S5†); it shifted to 4.90 ppm (peak b, Fig. 2) after formation of the 1,2,3-triazole units of PCTAz-T. Furthermore, the signal of the alkyne unit of PT (at 2.43 ppm) disappeared completely and the signal of the CH_2 group connected to the T unit (peak m, 4.57 ppm, Fig. S6†) shifted to 5.10 ppm after the click reaction, indicating the successful synthesis of the conjugated polymer PTCAz-T. Table 1 summarizes the molecular weight data of the conjugated polymers PTCAz-N_3 and PTCAz-T, determined through GPC analyses; the increase in the molecular weight upon proceeding from PTCAz-N_3 to PTCAz-T suggests that the side chain grafting had occurred.

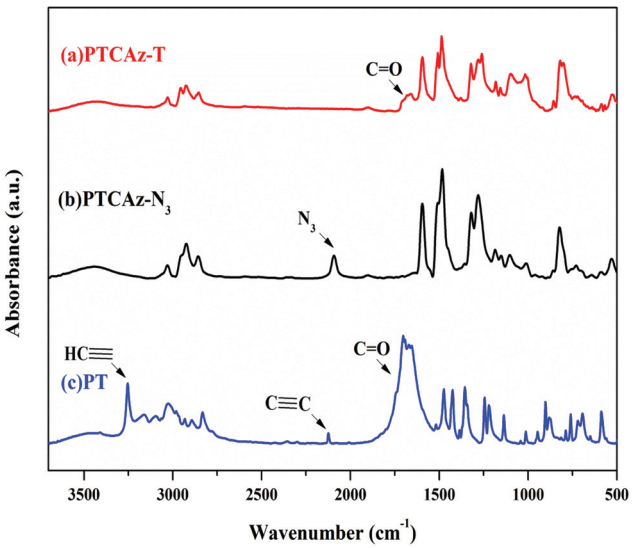

Fig. 1 FTIR spectra of (a) PTCAz-T, (b) PTCAz-N_3, and (c) PT, recorded at room temperature.

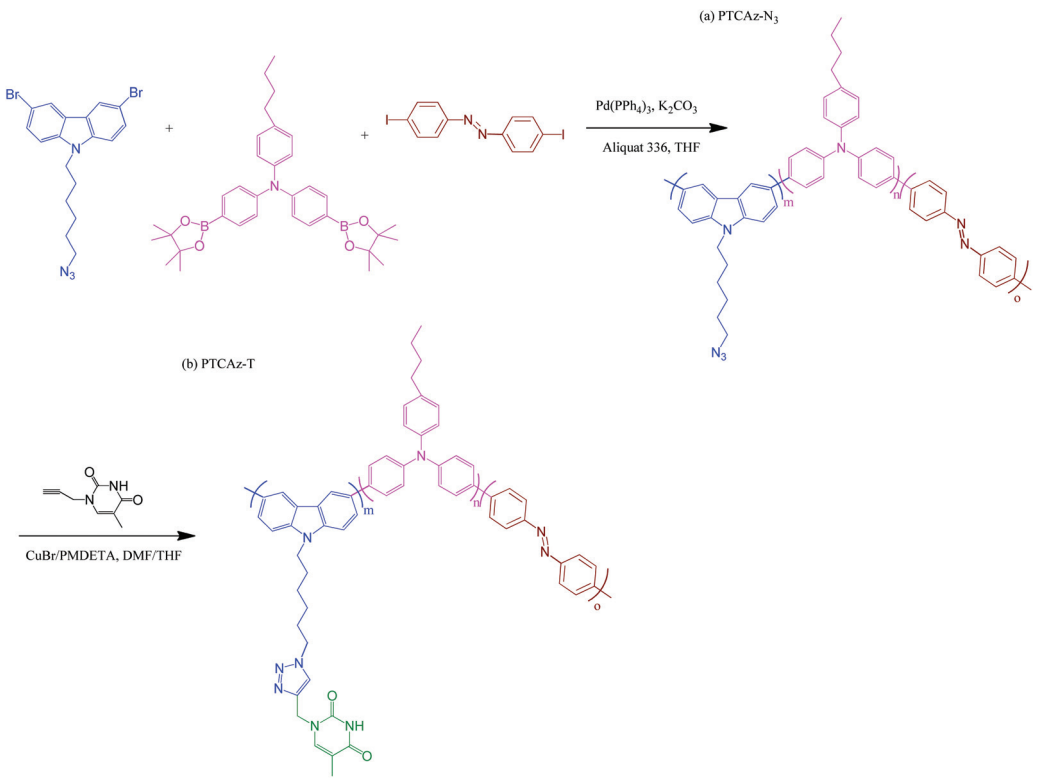

Scheme 1 Preparation of the conjugated polymers (a) PTCAz-N_3 (through Suzuki coupling polymerization) and (b) PTCAz-T (through click reactions of PTCAz-N_3 with PT).

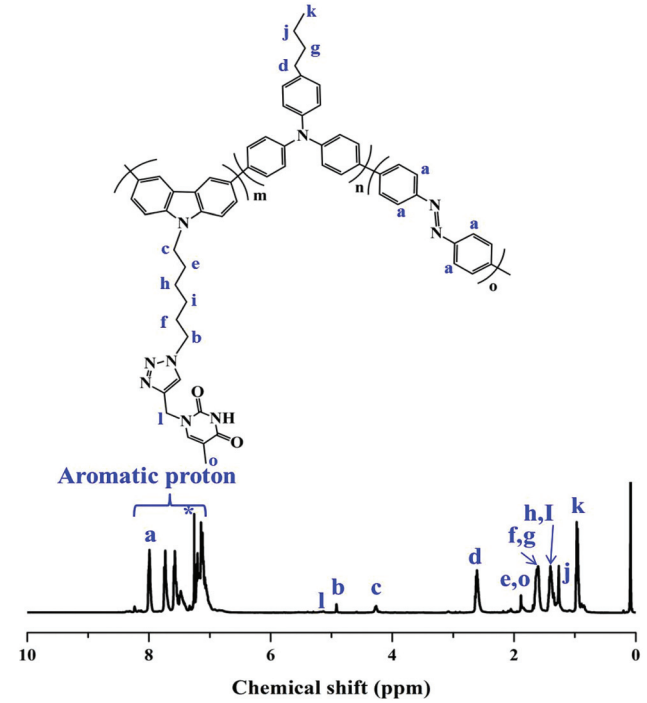

Fig. 2 ^{1}H NMR spectrum of the conjugated polymer PTCAz-T.

Table 1 Characterization data for the PTCAz-N_3 and PTCAz-T copolymers prepared in this study

Polymer	M_n	M_w	PDI
PTCAz-N_3-2 K[a]	2830	4130	1.46
PTCAz-T-2 K	2920	4180	1.43
PTCAz-N_3-4 K[a]	4170	6330	1.51
PTCAz-T-4 K	4750	6660	1.40
PTCAz-N_3-6 K[a]	6180	9400	152
PTCAz-T-6 K	7330	9800	1.34

[a] 2 K, 4 K, and 6 K indicate the molecular weight of the PTCAz-N_3 and PTCAz-T copolymers prepared in this study from GPC analyses.

Thermal properties of T-functionalized conjugated polymers

We used DSC to examine the thermal properties of the conjugated polymers PTCAz-N_3 and PTCAz-T (Fig. 3). We did not detect any obvious crystallization or melting peaks during the cooling or heating procedures, due to the poor packing ability of the triphenylamine units. The glass transition temperature of PTCAz-N_3 [129.5 °C, Fig. 3(a)] was higher than that of PTC-N_3 (109.4 °C),[30] presumably because of the extra rigid structure imparted by the azobenzene units in PTCAz-N_3. The value of T_g increased to 141.7 °C for PTCAz-T [Fig. 3(b)], suggesting that the strong T–T interactions [see Fig. 3(c)] restricted the molecular motion and, thereby, decreased the free volume. Such interactions would presumably also lead to a more stable morphology of the conjugated polymer PTCAz-T under relatively high temperatures.

Photoresponsivity of azobenzene-containing conjugated polymers

To examine the photoresponsivity of the conjugated polymers PTCAz-N_3 and PTCAz-T, we recorded their UV–Vis spectra before and after UV irradiation at 365 nm and measured the results until the photostationary states had been reached. Fig. 4 reveals that, for both PTCAz-N_3-4 K and PTCAz-T-4 K, the intensity of the absorbance at 445 nm (n–π*) decreased as a result of the *trans*-to-*cis* isomerization that occurred under UV irradiation at 365 nm for 1 min. The degree of isomerization (η) from the *trans* to the *cis* form was determined by using the equation $\eta = 1 - (A_s/A_0)$, where A_s and A_0 are the intensities of the absorbance at 445 nm for the photo-stationary and pristine states, respectively. The degrees of isomerization for the conjugated polymers PTCAz-N_3-4 K and PTCAz-T-4 K were 26.3 and 26.7%; thus, T-functionalization of the conjugated polymer had minimal effect on this value. This *cis* forms of the azobenzene units of PTCAz-N_3-4 K and PTCAz-T-4 K returned to their original *trans* forms after heating (50 °C) the polymers and placing them in the dark for 2 days. A quick *trans*-to-*cis* isomerization, but slow *cis*-to-*trans* isomerization, is typical of azobenzene-functionalized compounds.[31] Fig. 5 presents the PL spectra of the conjugated polymers PTCAz-N_3-4 K and PTCAz-T-4 K in dioxane (10^{-5} M), before and after UV irradiation at 365 nm. PTC-N_3 and PTC-T, the corresponding

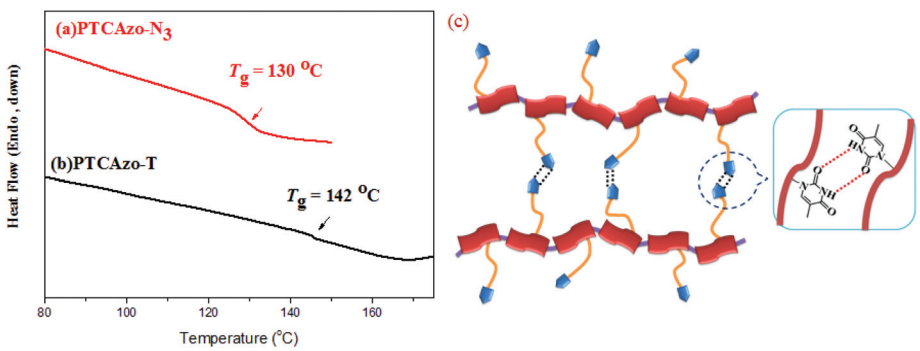

Fig. 3 (a, b) DSC thermograms of (a) PTCAz-N_3 and (b) PTCAz-T. (c) Schematic representation of the physical crosslinking, through T···T multiple hydrogen bonding interactions, of PTCAz-T.

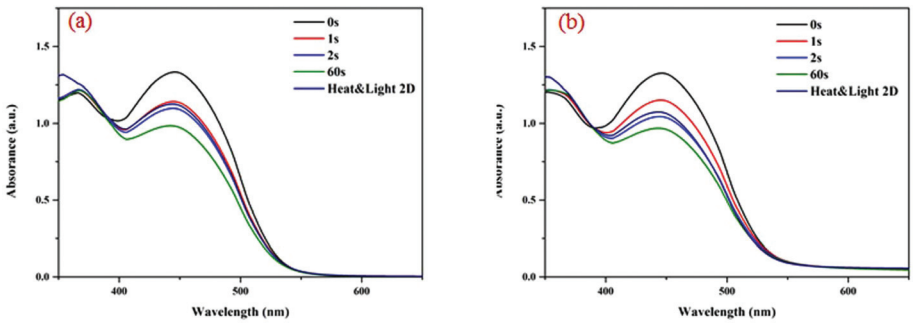

Fig. 4 UV–Vis spectra of the copolymers (a) PTCAz-N_3-4 K and (b) PTCAz-T-4 K after illumination with UV light (365 nm) for various lengths of time at room temperature and after standing in the dark at 50 °C for 2 days.

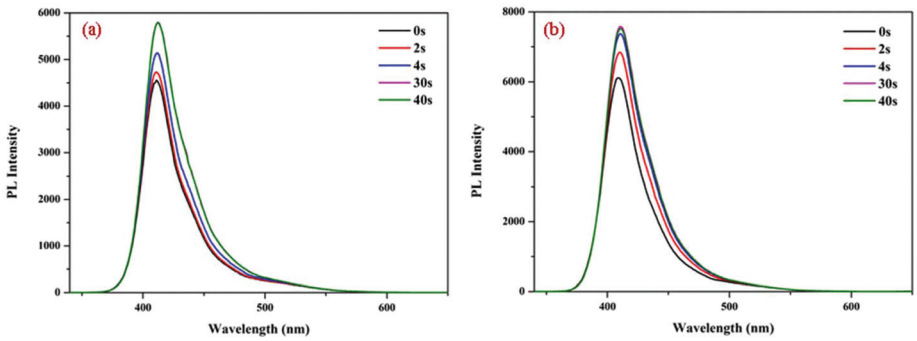

Fig. 5 PL spectra of the copolymers (a) PTCAz-N_3-4 K and (b) PTCAz-T-4 K after illumination with UV light (365 nm) for various lengths of time at room temperature.

polymers prepared without azobenzene units, displayed aggregation-caused quenching (ACQ) types of luminescence.[30] The PL intensity increased for both the conjugated polymers PTCAz-N_3-4 K and PTCAz-T-4 K after UV irradiation at 365 nm for only 40 s, indicating that the *trans*-to-*cis* isomerization enhanced the PL intensity. We suspect that the *cis* forms of the azobenzene units had greater difficulty packing than did the *trans* forms; thus, the ACQ phenomena decreased and then the PL intensity increased. Because the conjugated polymer PTCAz-T exhibited uniform photoresponsive behavior, we suspected that its supramolecular physically crosslinked network structure might display photochemical reversibility and the flexibility to design smart materials.

Photoinduced fabrication of SRGs from azobenzene-containing supramolecular conjugated polymers

To fabricate SRGs, we prepared transparent thin films of the conjugated polymers PTCAz-N_3 and PTCAz-T through a drop-coating method onto clean glass substrates [Scheme 2(a)]. The azobenzene-containing conjugated polymers presented clear spots after illumination with light from a polarized green laser (532 nm) for 30 min [Fig. 6(b)], implying that the refractive indices had changed. A one-dimensional diffraction pattern featuring strong fourth-order diffraction points was evident [Scheme 2(b)] after forming the grating. Fig. 6(c) and (f) display optical microscopy (OM) images of the SRGs formed

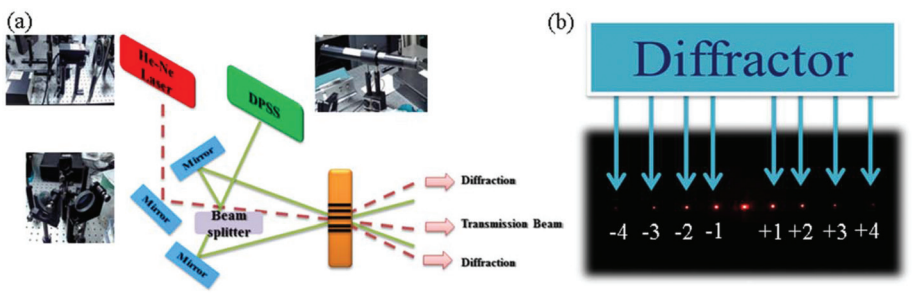

Scheme 2 (a) Experimental set-up for fabrication of SRG films. (b) Diffraction pattern of an SRG film probed with a laser beam.

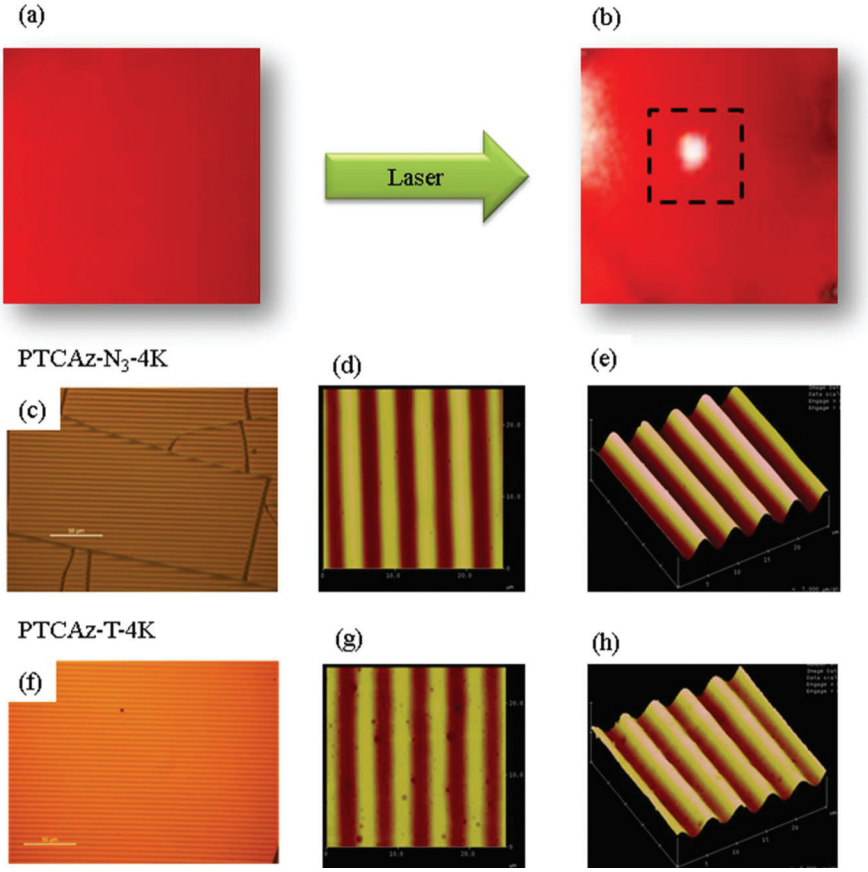

Fig. 6 (a, b) Photographic images of typical films of the copolymer PTCAz-T (a) before and (b) after exposure to laser light. (c, f) OM, (d, g) 2D AFM, and (e, h) 3D AFM images of films of (c–e) PTCAz-N_3-4 K and (f–h) PTCAz-T-4 K after exposure to laser light.

on the films of the conjugated polymers PTCAz-N_3-4 K and PTCAz-T-4 K, respectively. The grating pattern was clearly evident in the OM images measured 24 h after fabrication. The grating spatial period in the films of both PTCAz-N_3 and PTCAz-T was approximately 5 μm, with surface-modulation depths of 154 nm for the PTCAz-N_3-4 K film [Fig. 6(d) and (e)] and 86 nm for the PTCAz-T-4 K film [Fig. 6(g) and (h)], based on AFM imaging. Furthermore, the surface of the PTCAz-T-4 K film [Fig. 6(f)] was smoother than that of the PTCAz-N_3-4 K film, which had a cracked structure [Fig. 6(c)], suggesting that the strong T–T interactions provided a more stable morphology. The AFM images revealed the long-range order of an alternative lamellar structure, with bright lines being the crests of the waves from the *trans* form of the azobenzene unit and the dark lines being the valleys of the waves from the *cis* form. We determined the theoretical period length using the Bragg equation: $2d \sin\theta = n\lambda$, where n is equal to 1, λ is 532 nm for the polarized green light, and θ is the incident angle (3.5°) of the reference beam. The d-spacing of the theoretical period length of the interference fringe was 4.35 μm, close to the experimental result displayed in Fig. 6(d) and (g). We also examined the effects of different molecular weights of the conjugated polymers PTCAz-N_3 and PTCAz-T (Table 1) on their fabricated SRGs (Fig. 7). The surface-modulation depth decreased upon increasing of molecular weights of both PTCAz-N_3 and PTCAz-T. This behavior is consistent with the *trans*-to-*cis* isomerization becoming more difficult, and requiring more energy to reach completion, upon increasing the molecular weight of each azobenzene-containing conjugated polymer. Similarly, the surface-modulation depth of PTCAz-T was lower than that of PTCAz-N_3, because the strong T–T interactions further restricted the molecular motion and inhibited the *trans*-to-*cis* isomerization.

Grating stability is a key issue for holographic storage; the application of traditional azobenzene-containing polymers has, therefore, been restricted by their poor stability during storage, the result of relatively low values of T_g and their tendency to decompose over time. We suspected, however, that the multiple hydrogen bonding interactions of the homogeneous amorphous conjugated polymer PTCAz-T might make it suitable for holographic storage, because of its superior value of T_g. The physical crosslinking through multiple hydrogen bonding interactions did indeed result in a more fixed molecular orientation, resulting in the recorded film being stable after storage for at least six months under an ambient atmosphere. Fig. 8 displays the diffraction efficiencies for various diffraction orders in films of both PTCAz-N_3 and PTCAz-T after various recording times. The diffraction efficiency increased upon increasing the recording time, with

Copolymers	(a) PTCAz-N_3-2K	(b) PTCAz-N_3-4K	(c) PTCAz-N_3-6K
Average height of SRG (nm)	171	154	127
Height Profile of AFM image	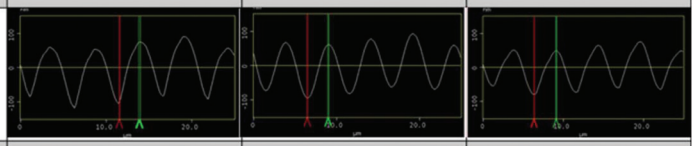		
Copolymers	(d) PTCAz-T-2K	(e) PTCAz-T-4K	(f) PTCAz-T-6K
Average height of SRG (nm)	97	86	76
Height Profile of AFM image	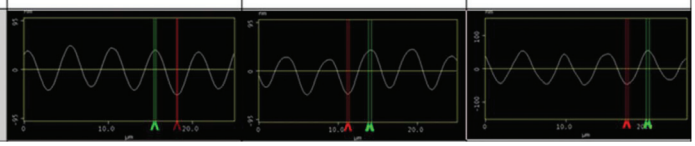		

Fig. 7 Height profiles in the AFM images of various PTCAz-N_3 and PTCAz-T copolymers after exposure to laser light.

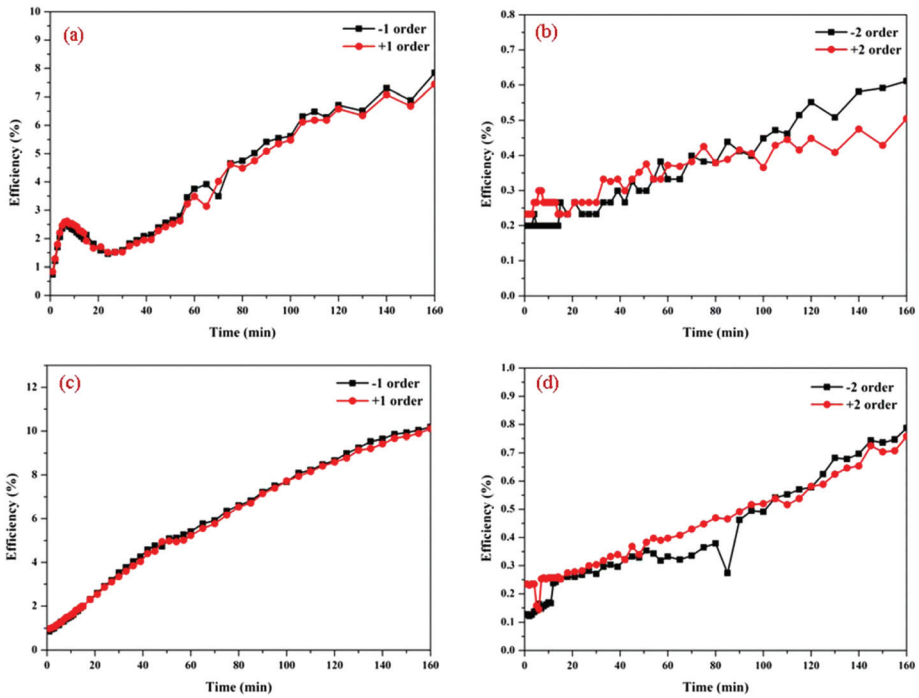

Fig. 8 Diffraction efficiencies of films of (a, b) PTCAz-N_3-4 K and (c, d) PTCAz-T-4 K after exposure to laser light: (a, c) first- and (b, d) second-order diffraction peaks.

that of the first order being higher than that of the second order, as expected. In addition, the diffraction efficiency for the first order of PTCAz-T-4 K (10.1%) was higher than that of PTCAz-N_3-4 K (7.8%) after recording for 160 min. These values are two to three times greater than the ones we had observed previously after using noncovalent bonding to attach azobenzene units to the side chains of amorphous polymers.[38] It appears that incorporating azobenzene units on the main chains of these amorphous conjugated polymers enhanced the surface-modulation depth during the *trans*-to-*cis* isomerization and, thereby, increased the diffraction efficiency. In addition to the combination of T and azobenzene units in the conjugated polymer resulting in stimuli-responsive behavior, the strong T–T interactions stabilized the surface morphology to such a degree that the *trans*-to-*cis* isomerization could be expanded to provide this real application of a supramolecular conjugated polymer.

Conclusions

We have successfully synthesized the T-functionalized, azobenzene-containing conjugated polymers through a combi-

nation of Suzuki coupling polymerization and a click reaction. This supramolecular azobenzene-functionalized conjugated polymer displayed enhanced thermal properties and possessed a stable morphology. Because azobenzene units were present in the main chains of these conjugated polymers, they underwent *trans*-to-*cis* isomerization when irradiated with laser light. Furthermore, we prepared SRG micro-patterns from our supramolecular azobenzene-functionalized conjugated polymer, with long-range order of the interference patterns, suggesting that they might have potential applications in optical storage media, while also suggesting new pathways for the development of supramolecular materials.

Conflicts of interest

There are no conflicts to declare.

Acknowledgements

This study was supported financially by the Ministry of Science and Technology, Taiwan, under contracts MOST 106-2221-E-110-067-MY3 and 105-2221-E-110-092-MY3. We thank Professor We-Hung Su for assistance with the fabrication of the SRGs.

References

1 C. H. Alarcon, S. Pennadam and C. Alexander, *Chem. Soc. Rev.*, 2005, **34**, 276–285.
2 F. Liu and W. M. Urban, *Prog. Polym. Sci.*, 2010, **35**, 3–23.
3 S. T. Zimmermann, D. W. R. Balkenende, A. Lavrenova, C. Weder and J. Brugger, *ACS Appl. Mater. Interfaces*, 2017, **9**, 41454–41461.
4 W. Lu, X. Le, J. Zhang, Y. Huang and T. Chen, *Chem. Soc. Rev.*, 2017, **46**, 1284–1294.
5 D. Wang, Y. Jin, X. Zhu and D. Yan, *Prog. Polym. Sci.*, 2017, **64**, 114–153.
6 P. Wang, H. L. Wang, Y. Fang, H. Li, J. H. He, J. Y. Ji, Y. Y. Li, Q. F. Xu, J. W. Zheng and J. M. Lu, *ACS Appl. Mater. Interfaces*, 2017, **9**, 32930–32938.
7 C. W. Huang, M. G. Mohamed, C. Y. Zhu and S. W. Kuo, *Macromolecules*, 2016, **49**, 5374–5385.
8 Y. C. Wu, B. P. Bastakoti, M. Pramanik, Y. Yamauchi and S. W. Kuo, *Polym. Chem.*, 2015, **6**, 5110–5124.
9 K. W. Huang, Y. R. Wu, K. U. Jeong and S. W. Kuo, *Macromol. Rapid Commun.*, 2013, **34**, 1530–1536.
10 W. H. Hu, K. W. Huang, C. W. Chiou and S. W. Kuo, *Macromolecules*, 2012, **45**, 9020–9028.
11 F. Ilhan, M. Gray and V. M. Rotello, *Macromolecules*, 2001, **34**, 2597–2601.
12 S. Chen, T. Yan, M. Fischer, A. Mordvinkin, K. Saalwachter, T. Thurn-Albrecht and W. H. Binder, *Angew. Chem., Int. Ed.*, 2017, **129**, 13196–13200.
13 G. Li, W. H. Chang and Y. Yang, *Nat. Rev. Mater.*, 2017, **2**, 17043.
14 M. S. Vezie, S. Few, I. Meager, G. Pieridou, B. Dorling, R. S. Ashraf, A. R. Goni, H. Bronstein, I. McCulloch, S. C. Hayes, M. Campoy-Quiles and J. Nelson, *Nat. Mater.*, 2016, **15**, 746–753.
15 H. K. Shih, Y. H. Chen, Y. L. Chu, C. C. Cheng, F. C. Chang and S. W. Kuo, *Polymer*, 2015, **7**, 804–818.
16 C. W. Huang, F. C. Chang, Y. L. Chu, C. C. Lai, T. E. Lin, C. Y. Zhu and S. W. Kuo, *J. Mater. Chem. C*, 2015, **3**, 8142–8151.
17 H. K. Shih, Y. L. Chu, F. C. Chang, C. Y. Zhu and S. W. Kuo, *Polym. Chem.*, 2015, **6**, 6227–6237.
18 E. Merino, *Chem. Soc. Rev.*, 2011, **40**, 3835–3853.
19 G. M. Mohamed, W. C. Su, Y. C. Lin, C. F. Wang, J. K. Chen and S. W. Kuo, *RSC Adv.*, 2014, **4**, 50373–50385.
20 M. G. Mohamed, C. H. Hsiao, F. Luo, L. Dai and S. W. Kuo, *RSC Adv.*, 2015, **5**, 45201–45212.
21 M. J. Hansen, M. M. Lerch, W. Szymanski and B. L. Feringa, *Angew. Chem., Int. Ed.*, 2016, **128**, 13712–13716.
22 S. L. Sin, L. H. Gan, X. Hu, K. C. Tam and Y. Y. Gan, *Macromolecules*, 2005, **38**, 3943.
23 X. Liao, G. Chen, X. Liu, W. Chen, F. Chen and M. Jiang, *Angew. Chem., Int. Ed.*, 2010, **122**, 4511–4515.
24 Z. Jiang, M. Xu, F. Li and Y. Yu, *J. Am. Chem. Soc.*, 2013, **135**, 16446–16453.
25 G. Liu, L. Zhou, Y. Guan, Y. Su and C. M. Dong, *Macromol. Rapid Commun.*, 2014, **35**, 1673–1678.
26 D. Brown, A. Natansohn and P. Rochon, *Macromolecules*, 1995, **28**, 6116–6123.
27 O. N. Oliveira Jr., D. S. dos Santos, D. T. Balogh, V. Zucolotto and C. R. Mendonca, *Adv. Colloid Interface Sci.*, 2005, **116**, 179–192.
28 A. Priimagi, J. Vapaavuori, F. J. Rodriguez, C. F. J. Faul, M. T. Heino, O. Ikkala, M. Kauranen and M. Kaivola, *Chem. Mater.*, 2008, **20**, 6358–6363.
29 A. Kravchenko, A. Shevchenko, V. Ovchinnikov, A. Priimagi and M. Kaivola, *Adv. Mater.*, 2011, **23**, 4174–4177.
30 J. Vapaavuori, C. G. Bazuim and A. Priimagi, *J. Mater. Chem. C*, 2018, **6**, 2168–2188.
31 Y. Zakrevskyy, J. Stumpe and C. F. J. Faul, *Adv. Mater.*, 2006, **18**, 2133–2136.
32 J. E. Koskela, J. Vapaavuori, J. Hautala, A. Priimagi, C. F. J. Faul, M. Kaivola and R. H. A. Ras, *J. Phys. Chem. C*, 2012, **116**, 2363–2370.
33 A. Natansohn and P. Rochon, *Chem. Rev.*, 2002, **102**, 4139–4176.
34 C. Barret, A. Natansohn and P. Pochon, *J. Phys. Chem.*, 1996, **100**, 8836–8842.
35 C. W. Huang, W. Y. Ji and S. W. Kuo, *Macromolecules*, 2017, **50**, 7091–7101.
36 Y. C. Wu, Y. S. Wu and S. W. Kuo, *Macromol. Chem. Phys.*, 2013, **214**, 563–571.
37 Y. C. Wu and S. W. Kuo, *Polym. Chem.*, 2012, **3**, 3100–3111.
38 C. W. Huang, P. W. Wu, W. H. Su, C. Y. Zhu and S. W. Kuo, *Polym. Chem.*, 2016, **7**, 795–806.

